Visualization study on the instabilities of phase-change heat transfer in a flat two-phase closed thermosyphon

XIA, Guodong, WANG, Wei, CHENG, Lixin and MA, Dandan

Published version

XIA, Guodong, WANG, Wei, CHENG, Lixin and MA, Dandan (2017). Visualization study on the instabilities of phase-change heat transfer in a flat two-phase closed thermosyphon. Applied Thermal Engineering, 116, 392-405.

Visualization study on the instabilities of phase-change heat transfer in a flat two-phase closed thermosyphon

Guodong Xia[a,*], Wei Wang[a], Lixin Cheng[a,b,*], Dandan Ma[a]

[a] College of Environmental and Energy Engineering, Beijing University of Technology, Beijing, 100124, China

[b] Faculty of Arts, Computing, Engineering and Science, Department of Engineering and Mathematics, Sheffield Hallam University, City Campus, Howard Street, Sheffield, S1 1WB, UK

[a,*] Corresponding author. Tel.: +86 10 67391985-8301; fax: +86 10 67391983.

[b,*] Corresponding author. Tel.: +44 114 2253103; fax: +44 114 2253100.

[a,*] Email addresses: xgd@bjut.edu.cn; [a,b,*] Email addresses: lixincheng@hotmail.com

Abstract: This paper presents systematic experiments and visualization on the instabilities of phase-change heat transfer for water, ethanol and acetone in a flat evaporator of a two phase closed system, respectively. The effects of the heat flux, filling ratio, coolant temperature and working fluid type on the instabilities and their mechanisms have been systematically investigated. The experimental results show that the instabilities of phase-change heat transfer are strongly related to the corresponding heat transfer modes. The instabilities of temperature and heat transfer coefficient (HTC) of the evaporator are mainly caused by the bubble behaviors, the physical properties and the operation pressures. Natural convection, intermittent boiling and fully developed nucleate boiling are the main heat transfer modes in the present study. The condensate droplets may affect the instabilities due to inducing periodic boiling at lower heat fluxes. The maximum standard deviations of the evaporator

temperature and vapor pressure fluctuations can reach 3.1 ^{o}C and 0.8 kPa respectively during the intermittent boiling. There is no intermittent boiling regime for ethanol and acetone in the present study. Therefore, no instability phenomena of nucleate boiling with ethanol and acetone are observed in the present study.

Key words: Instability; Phase-change heat transfer; Flat evaporator; Thermosyphon; Visualization study.

Nomenclature

C_p specific heat at constant pressure ($kJ \cdot kg^{-1} \cdot K^{-1}$)

FR filling ratio

h heat transfer coefficient ($kW \cdot m^{-2} \cdot K^{-1}$)

h_{fg} latent heat of vaporization ($kJ \cdot kg^{-1}$)

k thermal conductivity ($W \cdot m^{-1} \cdot K^{-1}$)

L length (m)

M relative molecular mass

N the total number of selected data

p pressure (kPa)

q heat flux ($W \cdot cm^{-2}$)

R surface roughness (μm)

T temperature (^{o}C)

t time (s)

ΔT wall superheat (^{o}C)

x distance (m)

Greek symbols

ρ density ($kg \cdot m^{-3}$)

σ surface tension ($mN \cdot m^{-1}$)

Subscripts

con	condenser wall
e	evaporator
i	item
in	inlet cooling water
l	liquid
r	relative
sat	saturation
SD	standard deviation
v	vapor
w	evaporator wall

1. Introduction

Phase change processes including boiling and condensation are widely used in many practical applications such as heat pipe, thermosyphon, various thermal energy systems and so on. It is thus essential to understand the fundamental phenomena involving boiling and condensation processes in order to design various heat transfer elements and thermal systems. In particular, new structure heat transfer devices such as flat heat pipe and thermosyphon are emerging in recent years. The interactions of boiling and condensation processes in such new structures and their effects on the boiling nucleation and bubble dynamics, heat transfer and temperature and pressure instabilities are urgent to be understood. For instance, a flat two-phase closed thermosyphon is an effective passive heat transfer device. It is an enclosed chamber filled with a certain amount of pure working fluid. Generally, it is placed between a small heat source and a large heat sink to achieve the uniform het flux and improve the performance of heat spreader. When heat is added in the evaporator section, the working fluid in the liquid pool vaporizes and carries heat from evaporator section to the condenser section, where heat is rejected into the heat sink by a condensation process. Then, the condensate falls back to the evaporator by gravity. Due to effective latent heat transfer associated with phase-change processes, it can transfer a large quantity of heat from the evaporator section to the condenser section with a relatively small temperature difference. Therefore, it is widely applied in various industrial fields, such as in heat exchangers, solar collectors, cooling of electronic components, de-icing and snow melting and so on [1]. However, for a two-phase closed thermosyphon, its application is always hindered by various limits such as dry-out limit for small filling ratio, entrainment limits for large filling ratio with high axial heat flux,

and boiling limit for large filling ratio with high radial heat flux. In addition to those limits, unstable phenomena of phase-change heat transfer in a two-phase closed thermosyphon often occur for large filling ratio with a low heat flux, such as intermittent boiling [2], pulse boiling [3] or geyser boiling [4]. Instabilities may cause problems in maintaining steady and safe operating of phase-change heat transfer devices. Therefore, instabilities of phase-change heat transfer in a two-phase closed thermosyphon are receiving more and more attention with the emergence of new structure devices involving phase change processes.

Instability of phase-change processes in a two-phase closed system is known as geyser boiling or intermittent boiling. This phenomenon often occurs in start-up process and operating process due to temperature excursion for a large filling ratio with a low heat flux. It was first investigated in thermosyphon by Griffith [5]. Geyser boiling occurs where liquid in a vertical tube with a closed end is heated near the bottom. Under certain thermal conditions, a large amount of liquid working fluid is periodically propelled from the evaporator to the condenser with a significant velocity due to the bubble's quick growth and expanding. This fast-moving liquid causes oscillating heat transfer and produces a characteristic sound in the two phase processes closed thermosyphon. When the superheated liquid and vapor bubbles reach the condenser, heat is rejected into the heat sink, collapsing the bubble and sub-cooling the condensate. Then, the condensate falls back to the evaporator by gravity and the geyser boiling continues. In an extreme condition, those processes may damage the container wall. This peculiar phenomenon is called as geyser boiling effect. Boure et al. [6] used the term of geysering for periodic expulsion and expulsion phenomena in a tube regardless of whether the tube is closed at the bottom. Geysering can be referred to as intermittent boiling in which

heat input is insufficient to maintain continuous nucleate boiling and thus cause unsteady processes such as temperature, pressure and heat transfer fluctuation accompanying various bubble behaviours in boiling processes. The geyser boiling occurs at the onset of nucleate boiling. Usually, the onset of boiling requires large temperature excursion. At a low heat flux, the onset of boiling can be delayed until the wall temperature reaches a certain superheat. This critical temperature is dependent on the fluid properties, the surface condition and other conditions of the system such as operating pressures and heat fluxes. Once the onset of boiling occurs, significant fluctuation of temperature and pressure are observed. The period of oscillation and the intensity of temperature and pressure fluctuations are two important parameters for the geyser boiling studies. The period of oscillation depends on the applied heat flux and the operating pressure, the geometry and orientation of the boiling surface, fluid types and the fluid properties. These influence factors may affect the geyser boiling, wall temperature, system operating pressure, bubble dynamics, heat transfer coefficient and the evaporation and condensation coexisting processes and systems.

Over the past decades, the effects of many parameters such as filling ratio, heat flux, inclination angle, kind of working fluid, aspect ratio, the temperature and mass flow of coolant, operating pressure on the geyser boiling and phase change instabilities have been studied. Both experimental and visualization studies have been performed. Negishi and Sawada [7] conducted an experimental study on the heat transfer of an inclined two-phase closed thermosyphon with water and ethanol as working fluids. The copper thermosyphon with and inside diameter of 13 mm and a length of 330 mm was employed with evaporator and condenser temperatures of 80 ^{o}C and 25 ^{o}C respectively. They observed that geyser

boiling occurred when the filing ratio is over 70%. Noie et al. [8] investigated the thermal performance of a two-phase closed thermosyphon with an outside diameter of 16 mm, an inside diameter of 14.5 mm, and a length of 1000 mm. They found that the geyser boiling occurred for filling ratio equal to or greater than 30% under normal operating conditions. To observe geyser boiling in a closed two-phase thermosyphon, Lin et al. [9] designed an annular thermosyphon with a vertical transparent outer tube for water and ethanol as working fluids. The effects of the heat load, condenser temperature, filling ratio and length of the evaporator on the characteristics of the geyser boiling were investigated in detail. At low heat load, the process of geyser boiling is clearly illustrated by flow visualization. At higher heat load, it occurs more frequently and irregularly. The wall temperature measure indicates that the period of geyser boiling is shorter at a higher load, a shorter evaporator length and a smaller filling ratio. Compared with water, the period is much more sensitive to heat load and the ranges of the heat load of the occurrence of the geyser boiling are much narrower for ethanol. A criterion was suggested for the occurrence of geyser boiling based on their data. Kunkoro et al. [10] performed a visualization study of geyser boiling in a two-phase closed thermosyphon with R113 and water as working fluids. The evaporator part is a 1507 mm vertical tube of 18 mm inside diameter and 22 mm outside diameter. By temperature and pressure measurements and visual observations, the mechanism of the geyser boiling was studied experimentally under various operating pressures and heat fluxes. They found out that temperature distribution or the internal-energy storage pattern may play an important role in initiating a geyser boiling. Temperature distribution is dependent on the geometry of the system, the physical properties of the working fluid and heat transfer process. They also

found that when superheat is the driving force in producing a geyser boiling, although during bubble generation the evaporator pressure may increase, geyser boiling may still occur. Imura et al. [11] conducted experimental studies on the conditions that led to the geyser boiling and developed boiling. They used the same dimensions of evaporator and condenser sections in a vertical two-phase closed thermosyphon and tested several cooling temperatures and heat flux for various filling ratios and working fluids. Sarmastiemami et al. [12] carried out experiments on the geyser boiling phenomenon in a two-phase closed thermosyphon. The effects of the inclination angle, filling ratio, input heat rate, mass flow rate of coolant, and inside diameter of the tube on a geyser boiling phenomenon have been discussed. The results show that the period of geyser boiling was longer for higher inclination angles and filling ratios. Furthermore, the geyser boiling did not occur for inclination angles of less than 15^{o}. Khazaee et al. [13] investigated experimentally the geyser boiling in a two-phase thermosyphon. Parameters such as filling ratio, aspect ratio heat input and the coolant mass flow rate affect the geyser boiling in thermosyphon. Two copper pipes of 1000 mm length with 15 mm and 25 mm inside diameter and methanol as the working fluid were employed. Their results showed that the period of geyser boiling decreased by increasing the heat load and aspect ratio and increased by increasing the filling ratio. Abreu and Colle [14] studied the effects of evaporator length, filling ratio, inclination angle, and cooling temperature on geyser boiling in solar heating two-phased closed thermosyphon. They found out that the heat flux is the most important parameter in the determination of boiling regimes. Farsi et al. [15] observed the temperature excursion and fluctuation at start-up period of the two-phase closed thermosyphon. Similar phenomena on the closed thermosyphon solar collectors were

observed by Abreu and Colle [14]. Kafeel and Turan [16] studied the effect of different pulsed increases of the heat input at the evaporator zone on the behaviour of the thermosyphon. Fadhl et al. [17] built a CFD model to simulate the details of the two-phase flow and heat transfer phenomena during the start-up and steady-state operation of the thermosyphon. Jouhara et al. [18] proposed a three-dimensional CFD simulation which has successfully predicted and visualised, for the first time, a flow pattern that take place with water at low power throughput, known as geyser boiling. The heat throughput has a significant effect on the characteristics of the geyser boiling in which the geyser boiling phenomenon does not appear for higher heat throughput. The geyser boiling simulations have been visually validated with a transparent glass thermosyphon experiment.

From the foregoing literature review, it is clearly seen that most of the available studies concern about the phase change processes in a conventional two-phase closed thermosyphon which is a long tube with a small inside diameter and positioned vertically. Compared to a conventional two-phase closed thermosyphon, a flat two-phase closed thermosyphon is a novel thermosyphon which has larger inside diameter and shorter length. Its evaporator and condenser are both positioned horizontally. Therefore, the phase change heat transfer characteristics and mechanisms may different from those in the conventional thermosyphon systems due to the different structures and arrangement. The bubble behaviours and boiling regimes may be different and thus affect the instabilities in the boiling process. The intermittent boiling regime rather than geyser boiling regime may occur in the evaporator of a flat two-phase closed thermosyphon because the bubble departure diameter is much smaller than the inside diameter and can’t propel a large amount of working fluid from the evaporator

to the condenser. Recently, several researchers conducted experiments on the phase change heat transfer performance in plate two-phase closed thermosyphon [19], vapor chamber [20] and small confined space [21]. Zhang [19] and Peng [20] reported that heat transfer devices start up suddenly and the temperatures fluctuate in a certain range. Zhang [21] introduced pressure standard deviation (*SD*) as an indicator to estimate the intensity of the disturbance of vapor and liquid. Results show that the *SD* of pressure increase from 0.5 to 0.8 kPa with increasing of heat flux. The influences of liquid levels and enhanced structures on the heat transfer performance of flat two-phase closed thermosyphon also have been studied [22,23]. They have reported that the temperature and pressure fluctuations in various phase-change heat transfer devices during the start-up and steady operational periods. However, the fluctuations of heat transfer mechanisms and the effects parameters are still not well understood and need to be further investigated through systematic experiments and new visualization on the phase change processes. Furthermore, the effects of various parameters on the boiling heat transfer processes in an evaporator and condenser coexisting system is not well understood. In particular, the effects of the bubble origination, growth and departure on the temperature and pressure and heat transfer fluctuations. Therefore, the objectives of this work are to study experimentally the instabilities of phase-change phenomena in a flat two-phase closed evaporator and condenser coexisting system with three working fluids of water, ethanol and acetone under sub-atmospheric pressures and to visualise the phase change processes including bubble behaviours, condensate droplet behaviours and their effects on the boiling processes with a high speed camera in order to understand the mechanisms.

2. Experimental apparatus, test section and measurement system

The experimental system mainly consists of an experimental apparatus, a test section and a measurement system which are described respectively here.

2.1. Experimental apparatus

In order to study the instabilities of nucleate boiling processes and their mechanisms in a flat two-phase closed evaporator condenser coexisting system, an experimental apparatus was designed and constructed. Fig 1 shows the schematic diagram of the experimental system. It consists of a cooling system (1), a test section (2), a heating unit (3), a transformer (4), a data acquisition (5), pressure transducer (6) a vacuum pumping and filling system including a reservoir (7), a drainage bottle (9) and a vacuum pump (10), a high speed camera (8) and a PC (11). The test section is a chamber mainly including a flat evaporator and a flat condenser (details are given in Figs. 2 and 3 and described in the next paragraph). Heat is supplied to the test section by electrical heating and heat conduction. Then the heat was transferred to the working fluid to achieve nucleate boiling in the flat evaporator and dissipated by the cooling water via a condenser. The working fluids are distilled water, ethanol and acetone respectively and were boiled in the flat evaporator of the test section. The heat flux was controlled by adjusting the output voltage of a transformer. A chiller with an accuracy of 0.1 K was employed to circulate the cooling water through the flat condenser to remove the heat and condensate the vapor. The high speed camera was used to visualise the phase change processes occurred in the test section. The data acquisition system was used to record the measured parameters such as temperatures and pressures. The PC was used to store the experimental data and images.

Fig. 2 illustrates schematically the details of the assembly of the heating unit in the lower part and the test section in the upper part. The heating unit is a copper rod with four cartridge electric heaters. The heating unit is contacted with the flat evaporator and the heat is transferred to the flat evaporator through thermal conduction. The copper rod diameter is 40 mm at the lower part and 20 mm at the upper part. To reduce the heat loss from the heater, the outside of the copper rod was well insulated by insulation material. To obtain a steady state temperate distribution along the axial direction, three thermocouples were installed along the central axis of the copper rod as indicated as T_1, T_2 and T_3 in Fig. 2. The thermometer holes were 10 mm in depth and 1 mm in diameter at located at 3, 13 and 23 mm from the top surface of the copper rod as illustrated in Fig. 3.

2.2. Test section

The test section was illustrated in the upper part of the diagram in Fig. 2. It is a flat two-phase closed system which consists of two disk-shaped flat copper plates used as an evaporator and a condenser respectively and a quartz tube used as sidewall. Fig. 3 shows the detailed dimensions of the evaporator and the condenser. The internal chamber of the test section has a diameter of 80 mm and a height of 60 mm which is also the distance between the evaporator and the condenser. The quartz tube is used to observe the heat transfer process and it has an outside diameter of 90 mm, a thickness of 5 mm and a height of 40 mm. The contact parts are between different pieces sealed with Viton O-rings. A thermocouple was embedded in the middle of the flat evaporator. The top surface temperature of the evaporator wall was then calculated using one dimensional Fourier's law of heat conduction under the steady condition.

2.3. Measurement system

The measurement system consists of a number of thermocouples, a pressure transducer, a data acquisition unit, a high speed video camera and a PC. The main measurement parameters are the axial temperatures in the heating copper rod T_1, T_2 and T_3, the temperature inside the flat evaporator, the temperature of the working fluid, the vapor temperature and three temperatures inside the flat condenser, the pressure in the test chamber as shown in Figs. 2 and 3. Nine calibrated T-type thermocouples with shields (1 mm in diameter) are used to measure temperatures at selected positions with an accuracy of ± 0.1 K. To obtain the wall temperatures of the flat evaporator and condenser, thermocouples T_4, T_5, T_6 and T_9, T_{10}, T_{11} are arranged in the evaporator and condenser and shown in Fig.3. Thermocouples T_7 and T_8 are used to measure the liquid and vapor temperatures in the tests. To reduce the contact thermal resistance and the temperature measurement error, high conductivity grease is laid between the heating surface and the evaporator and in the holes. The flat evaporator and the heating unit are tightened with screws. An absolute pressure transducer is located at the upper part of the test chamber as indicated in Fig. 2. Its accuracy is 0.25% for an operating range of 0-10^5 Pa. The high speed video camera (Motion Pro X4 plus) is used to visualize the boiling and condensation processes. All measured parameters and images are taken by the Agilent 34970A data acquisition system every second and stored in the PC for future data reduction and analysis.

3. Data reduction methods, uncertainty analysis and test procedure

3.1. Data reduction methods

With the three measured temperatures T_1, T_2 and T_3 in the axial direction of the heating copper rod in Fig. 2, the heat flux is calculated based on one-dimensional steady heat conduction equation as

$$q = -k\, dT/dx \tag{1}$$

where k is the thermal conductivity of pure copper, dT/dx is the temperature gradient in the heating rod to the working fluid.

Based on the method of temperature measurement of Tang [24] and Zhang [25], three thermocouples T_4, T_5 and T_6 are installed in the evaporator wall. The difference between T_4, T_5 and T_6 is found to be within 0.5 ^{o}C in all cases, thus the evaporator wall temperature is uniform. The top surface temperature of the evaporator wall T_w is calculated according to the one-dimensional Fourier law

$$T_{ave} = \frac{T_4 + T_5 + T_6}{3} \tag{2}$$

$$T_w = T_{ave} - q\frac{L}{k} \tag{3}$$

where T_{ave} is the average temperature of T_4, T_5 and T_6, L is the distance between the thermocouple T_4 and the top surface of the evaporator wall. Similarly, the low surface temperature of the condenser wall T_{con} also can be calculated by the same methods.

The evaporator wall superheat ΔT is defined as

$$\Delta T = T_w - T_l \tag{4}$$

where T_w is the top surface temperature of the evaporator, T_l is the bulk liquid temperature and is equal to the saturated temperature T_{sat}. With the known local heat flux and wall superheat, the transient heat transfer coefficient is determined with the equation below:

$$h = q/(T_w - T_l) \tag{5}$$

The average wall superheat and heat transfer coefficient are defined as

$$\Delta\bar{T} = \overline{T_w} - \overline{T_l} \tag{6}$$

$$h_{ave} = q_{ave}/(\overline{T_w} - \overline{T_l}) \tag{7}$$

where $\overline{T_w}$ and $\overline{T_l}$ are the average value of heating surface and bulk liquid for 12 minutes after the system reached its steady-state, the q_{ave} is determined from Eq.(1).

In order to estimate the intensity of the temperature, pressure and heat transfer coefficient fluctuations, the standard deviation (*SD*) was introduced. These *SD*s are calculated for 12 minutes when the system reached its steady-state. The *SD* is defined by the following equation:

$$SD = \sqrt{\frac{1}{N}\sum_{i=1}^{N}(X_i - \bar{X})^2} \tag{8}$$

Therefore, under the steady-state conditions, *SD* is an accurate description of temperature, pressure and heat transfer coefficient fluctuations.

3.2. Uncertainty analysis

Using a standard error analysis [26], the uncertainty of heat flux is determined as

$$\frac{\Delta q}{q} = \sqrt{\left(\frac{\Delta k}{k}\right)^2 + \left(\frac{\Delta \delta T}{\delta T}\right)^2 + \left(\frac{\Delta \delta x}{\delta x}\right)^2} \tag{9}$$

According to the average temperature of copper block, k is determined from the standard physical properties table and its relative error $\Delta k/k$ can be neglected. The calibrated error of the T-type thermocouples is about ±0.1 K. In the testing range, the uncertainty of the heat flux is estimated to be about 8.5%.

The uncertainly of heat transfer coefficient is determined as

$$\Delta h = \sqrt{\left(\frac{\partial h}{\partial q}\right)^2 \Delta q^2 + \left(\frac{\partial h}{\partial T_w}\right)^2 \Delta {T_w}^2 + \left(\frac{\partial h}{\partial T_l}\right)^2 \Delta {T_l}^2} \tag{10}$$

Thus the relative uncertainty can be deduced by substituting Eq. (5) to Eq. (10) as:

$$\frac{\Delta h}{h} = \sqrt{\left(\frac{\delta q}{q}\right)^2 + \left(\frac{\Delta T_w}{T_w - T_l}\right)^2 + \left(\frac{\Delta T_l}{T_w - T_l}\right)^2} \tag{11}$$

where Δq, ΔT_w, and ΔT_l are the uncertainties of heat flux, wall surface temperature and pool liquid temperature. The maximum uncertainty of heat transfer coefficient is obtained by a smaller surface temperature and a larger pool liquid temperature. The maximum relative uncertainty of heat transfer coefficient is 9.3%.

3.3. Test procedure

First, before filling the working fluids into the test chamber, the tube was completely cleaned to remove any grease or oil from the inner surface. The boiling and condensation surface conditions may strongly influence the phase-change heat transfer process. Therefore,

the surfaces were first polished by emery paper (No. 5000) and then washed in sequence by distilled water, ethanol, acetone and distilled water.

Then, a selected amount of degassed working fluid was filled into the test chamber after it was evacuated down to a pressure of 3.8×10^{-4} Pa. After that, the vapor chamber was evacuated again. To test the tightness, it was left under the room conditions for 24 hours, and if the measured pressure in the test section was equal to the saturated pressure of the vapor temperature within 5%, then the chamber can be considered leak tight during the experiments.

Next, a series of experiments were performed to investigate of the instabilities of nucleate boiling in the two-phase closed test section for three working fluids at specified conditions. The working fluids are water, ethanol and acetone respectively. Table 1 shows the thermal physical properties for the same saturation temperature of 20 ^{o}C. The control parameters are the heat flux, the filling ratio and the inlet temperature of the cooling water. The test heat flux is from 13.1 to 93 W·cm^{-2}. The filling ratio was from 10% to 90%. The temperature of the cooling water was set at 12 ^{o}C, 16 ^{o}C and 20 ^{o}C. For each case, the temperature and pressure were measured. The effects of the heat flux, filling ratio and cooling water temperature were investigated in detail for the distilled water as working fluid at first. In order to identify the working fluids and thermal physical property effects, experiments on the boiling instabilities with ethanol and acetone were conducted. Typical boiling processes were recorded by the high speed video camera.

4. Experimental results and analysis

According to the experimental data and visualisation observation, the effects of heat flux, filling ratio, cooling water temperature and working fluid types on the instabilities of nucleate boiling processes in the two phase closed test section are analysed here. Visualisation study using the high speed video camera was performed to understand the mechanism of the instabilities of nucleate boiling heat transfer in the flat two-phase closed system. With combined visualization and parametric trends of temperature and pressure, the bubble behaviour and the instabilities of phase-change heat transfer processes together with their mechanisms with various control parameters are explored.

4.1. The Effect of heat flux on the instability of nucleate boiling heat transfer

In this section, a series of experiments were performed for distilled water at different heat fluxes. The filling ratio and inlet cooling water temperature are 50% and 12 ^{o}C respectively.

Fig. 4 shows the transient temperature response of the evaporator wall for water boiling at four different heat fluxes 13.1, 38.7, 47.4 and 80.2 W·cm^{-2}. At the heat flux of 13.1 W·cm^{-2}, only natural convection occurs and no nucleate boiling phenomenon appears. With increasing the heat flux, the temperature of evaporator starts to fluctuate due to the incipience of boiling. This wall temperature instability is caused due to the heat transfer coefficient of evaporator wall repeated change of between natural convection and nucleate boiling. It is also observed that incipience of boiling at a higher heat flux is faster than that at a lower heat flux. The fluctuation of temperature increases from 0.8 ^{o}C to 2.8 ^{o}C and then decreases to 0.5 ^{o}C with increasing heat flux. These variation trends can be explained according to boiling heat

transfer mechanisms and corresponding bubble characteristics at the given heat flux. With increasing the heat flux, the number of active nucleation sites on the evaporator wall increases. The activation and inactivation of the nucleation sites at a moderate heat flux result in an intermittent boiling phenomenon which causes large temperatures and pressure fluctuations.

Fig. 5 shows typical variations of the several measured temperatures (evaporator wall T_w, liquid T_l, vapor T_v and condenser wall temperatures T_{con}) and saturated pressure p_{sat} of the two phase closed test section with time for water at a heat flux of 13.1 $W \cdot cm^{-2}$. The variation trends of the wall temperature of the flat evaporator and water temperature with time are similar and the variation trends of the temperature of vapor and the saturation pressure of vapor are similar. However, their variation trends show opposite direction. The trend of the condenser wall temperature is relatively steady. The maximum intensities of fluctuations of the evaporator wall temperature and vapor pressure are 0.8 ^oC and 0.3 kPa, respectively. It can be observed that the period of the boiling process was short while the natural convection process was long. Variations of the corresponding transient heat transfer coefficient and wall superheat degree versus time are shown in Fig. 6a and 6b. It can be seen that fluctuations of the heat transfer coefficient and the wall superheat degree are obvious. The average heat transfer coefficient and its maximum intensity of its fluctuation are 8.58 and 0.72 $kW \cdot m^{-2} \cdot K^{-1}$, respectively. In order to understand these instabilities, the high speed video camera was used to observe the heat transfer process as shown in Fig. 7. The main heat transfer mode between the flat evaporator wall and water is natural convection because no bubble generation was observed on the wall. However, an interesting phenomenon is that an isolated bubble was

observed inside the water although no nucleation site was activated on the evaporator wall. From these images in Fig. 7, it is obvious that the isolated bubble was generated due to the dripping of the condensate droplet into the water which may be superheated liquid. Fig. 7a shows the quiescent surface of the liquid in the chamber before the dripping of a condensate droplet. Figs. 7b to 7l show a condensate droplet drops into water and the droplet induces the generation of the isolated bubble. In this process, the quiescent flat surface of liquid pool partially concaves downward due to the effect of condensate liquid droplet. The bubble will be captured during the resuming of liquid level and can act as nucleation site. The heat transfer modes are mainly conduction and natural convection. Therefore, the fluctuation of the temperatures and pressure are small. The fluctuation of heat transfer coefficient is caused by the periodic isolated bubble generation, growth, movement and breakup. This process generates the agitation of the liquid which may enhance the natural convection. The growth of bubble absorbed the latent heat of the superheat liquid absorbed, thus the heat transfer coefficient of the evaporator wall increases. The combined effects simultaneously decrease the temperature of the evaporator wall and water. In the same time, the periodic bubble grows, moves up and pushes the liquid on the top of the bubble upward, which generates the fluctuations of the temperature and pressure of vapor. Therefore, the instabilities of boiling heat transfer in the two phases closed test section caused by the periodic dripping of the condensate droplet which induces the periodical boiling for this low heat flux.

Fig. 8 shows typical variations of the several measured temperatures and saturated pressure of the two phase closed test section with time for water at a heat flux of 38.7 $W \cdot cm^{-2}$. The variation trends of the wall temperature of the flat evaporator and water temperature with

time are similar and the variation trends of the temperature of vapor and the saturation pressure of vapor are similar. However, their variation trends show opposite direction. The trend of the condenser wall temperature fluctuates slightly. The maximum intensity of the fluctuations of evaporator wall temperature and the vapor pressures are 2.8 ^{o}C and 0.8 kPa, respectively. The maximum intensity of the vapor pressures is equal to the experimental result of Zhang [18]. At a higher heat flux q = 38.7 W·cm^{-2}, the heat transfer mode and mechanisms are quite different from the observed phenomena of a lower heat flux q = 13.1 W·cm^{-2}. Variations of the corresponding transient heat transfer coefficient and wall superheat degree versus time are shown in Figs. 9a and 9b. It is obvious that the intensities of fluctuations of the heat transfer and wall superheat degree become stronger as compared to those in Figs.6a and 6b at a lower heat flux. The average heat transfer coefficient and its maximum intensity of fluctuations are 12.02 and 1.57 kW·m^{-2}·K^{-1}, respectively. The intermittent boiling with bubble initiation, growth, and departure periodically is observed at this higher heat flux as shown from Figs. 10a to 10f in. Both natural convection and intermittent boiling are the heat transfer modes. Thus, the intensities of the fluctuations of the evaporator wall and water temperatures become strong due to the combined function of nucleate boiling and natural convection. The critical wall temperature and the evaporator wall temperature which causes the maximum fluctuation are approximate 55 ^{o}C. Once the nucleate boiling occurs, the temperatures of the evaporator wall and water decrease due to the high heat transfer coefficient. The high heat transfer coefficient is attributed to the behaviour of bubble which results in micro-layer evaporation at the bottom of the bubble, the micro

convection, the phase-change of liquid-vapor interface of the bubble and the transient conduction due to the wake effect of the bubble departure.

The first frame (Fig.10a) shows the origination of bubble, and then the heat transfer modes will change from natural convection to nucleate boiling. The series of frames show a typical bubble behaviour at the mediate heat flux. Obviously, there is only one nucleation site is activated each time. The effect of dripping of the condensate droplet which induces the boiling for this mediate heat flux was not observed and therefore, it has no effect on the boiling process.

Fig.11 shows typical variations of the several measured temperatures and saturated pressure p_{sat} of the two phase closed test section with time for water boiling at a heat flux of 80.3 $W \cdot cm^{-2}$. With further increasing the heat flux, the wall superheat increases and more nucleation sites are activated. The waiting period became much short. The nucleate boiling mechanism is evolved from intermittent boiling into fully developed nucleate boiling. It can be seen from Fig. 11 that intensities of the fluctuations of temperatures and pressure becomes smaller as compared to those in Fig. 8. The maximum intensity of fluctuations of the evaporator wall temperatures and the vapor pressures are 0.5 ^{o}C and 0.2 kPa, respectively. Variations of the corresponding transient heat transfer coefficient and wall superheat degree versus time are shown in Figs. 12a and 12b, respectively. It is obvious that the intensities of fluctuations of the heat transfer and wall superheat degree become weaker as compared to those in Figs. 6a and 6b at a medium heat flux but become stronger than those in Fig. 6a and 6b at a lower heat flux. The average heat transfer coefficient and the maximum intensity of its fluctuations are 20.52 and 1.04 $kW \cdot m^{-2} \cdot K^{-1}$, respectively. This is mainly due to the developed

nucleate boiling mode as shown in Figs. 13a to 13f. The heat transfer becomes strong and relatively steady. Therefore, the temperatures of the flat evaporator wall and water have small fluctuations. When the bubbles depart and burst, the upper vapor space becomes large, but new bubbles initiation and growth during the last bubble departure to inhibition the decreasing of the vapor space at same time as shown in Fig. 13. Therefore, the fluctuations of the temperatures of vapor and condenser, and the pressure of vapor also are small.

For the three selected heat fluxes of 13.1, 38.7 and 80.2 $W \cdot cm^{-2}$, the instabilities of nucleate boiling heat transfer are strongly related to the corresponding heat transfer modes and mechanisms at different heat fluxes. Natural convection, intermittent boiling and fully developed nucleate boiling are observed from lower heat flux to high heat flux in the experiments and visualisations. The periodical variation of heat transfer due to the bubble behaviours leads to the instabilities of nucleate boiling heat transfer in the two phase closed system. The condensate droplets may significantly affect the instabilities in the natural convection heat transfer mode due to the inducing of isolated bubble in the liquid but has little effect in intermittent boiling and fully developed nucleate boiling modes.

4.2. The effect of the filling ratio (*FR*) on the instabilities of nucleate boiling heat transfer

Fig. 14 shows the *SD* of the evaporator wall temperature versus heat flux for water boiling at *FR* = 10, 30, 50, 70 and 90%. It indicates the effect of the filling ratio of water as the working fluid on the instabilities of nucleate boiling heat transfer at various heat fluxes. It can be seen that the maximum temperature fluctuations occur in the range from 23.6 to

69.6 W·cm^{-2}. The filling ratio has a significant effect on the instabilities when the heat flux is less than 69.6 W·cm^{-2}, but has little effect when the heat flux is higher than 69.6 W·cm^{-2}. From the visualization, it can be concluded that the maximum temperature fluctuation occurs in the intermittent boiling regime. The effects of the filling ratio vary with the heat flux due to the different heat transfer modes as discussed in section 4.1. In the intermittent boiling regime, the bubble intermittently initiates, grows, departures and bursts. As the filling ratio increase, the departure radius and the floating speed increase due to the high liquid level and large buoyancy. In the meantime, the wake effect of the departing bubble is enhanced. That will further decrease the temperature of evaporator wall to deactivate the nucleation sites. Therefore, the fluctuations of evaporator wall temperature increases with increasing the filling ratio at q = 38.7 W·cm^{-2} and are the maximum as compared to the other two heat fluxes. The fluctuation of temperature varies from 1.2 ^{o}C to 3.1 ^{o}C. At a higher heat flux, the fluctuation of the evaporator wall temperature decreases with increasing the filling ratio because the fully developed boiling regime is prevailing and the thermal inertia of bulk liquid increases with increasing the filling.

4.3. The effect of the inlet cooling water temperature on the instabilities of nucleate boiling heat transfer

Fig. 15 shows the *SD* of evaporator wall temperature versus heat flux at three inlet cooling water temperatures of 12 ^{o}C, 16 ^{o}C and 20 ^{o}C for nucleate boiling of water at *FR* = 50%. It indicates the effect of inlet cooling water temperature on the instabilities of nucleate boiling heat transfer in the two phase closed system. It can be seen that the inlet cooling water temperature has no effect on the temperature fluctuations when the heat flux is less than 23.6

$W \cdot cm^{-2}$. The reason is because the heat transfer is in the natural convection mode. When the heat flux is higher than 23.6 $W \cdot cm^{-2}$, the effect of the inlet cooling water temperature becomes obvious. The intensities fluctuations become strong at heat fluxes from 23.6 to 69.6 $W \cdot cm^{-2}$ which are actually in the intermittent boiling regime as discussed in section 4.1. There are also peak values of the fluctuations indicated by the *SD* in Fig. 15 which are in fact in the intermittent boiling regime. The fluctuations of the evaporator wall temperature decreases with increasing the heat flux after reaching the peak values. At a heat flux higher than 69.6 $W \cdot cm^{-2}$, the fluctuations become weak as compared to the medium heat fluxes. This is mainly because the heat transfer mode is in the fully developed nucleate boiling regime.

4.4. The effects of the working fluid types on the instabilities of the nucleate boiling heat transfer

Fig. 16a shows the *SD* of the evaporator wall temperature versus heat flux for boiling of three different working fluids: distilled water, ethanol and acetone at *FR* = 50% and inlet cooling water T_{in} = 12 ^{o}C. It displays the effects of working fluid types on the instabilities of nucleate boiling heat transfer in the two phase closed system. The instabilities are obvious for the nucleate boiling of water and the maximum fluctuation of the wall temperature can reach 3.1 ^{o}C while there are no instabilities for the nucleate boiling of ethanol and acetone because the fluctuations of evaporator wall temperatures for ethanol and acetone are approximate 0.2 ^{o}C.

Fig. 16b shows the boiling curves for three different working fluids. The heat transfer coefficients of water are greater than those of ethanol and acetone. Furthermore, the experimental results were compared to the Cooper nucleate boiling correlation [27] which is expressed as

$$h = \frac{55 p_r^{(0.12-0.2\log_{10} R)} q^{2/3}}{\sqrt{M}(-\log_{10} p_r)^{0.55}} \quad (12)$$

where p_r is the reduced pressure, R is the surface roughness, M is the relative molecular mass. Since the surface roughness has a significant effect on the boiling heat transfer of water at low reduced pressure, the copper surface roughness was measured to account for this effect when using Eq. (12). The measured surface roughness is 0.99 μm. As shown in Fig.16c, the deviation of HTC at various heat fluxes between experimental results and predictions within 30%, 15% and 10% for distilled water, ethanol and acetone, respectively. The small deviations for ethanol and acetone show the experimental system has a good performance with high reliable. The large deviation for distilled water means that the confined space could result in more influence because the bubble departure diameter of distilled water is larger at sub-atmospheric pressure than that of at atmospheric pressure. The bubble behavior has a significant effect on the heat transfer performance.

For different working fluids, these instabilities are mainly affected by the different heat transfer modes, physical properties and bubble behaviour. From Table 1, it can be seen that the surface tension of water is much larger than those of ethanol and acetone. The larger surface tension makes it is more difficult for the bubbles to depart and thus the departure frequency of the bubbles becomes less. Furthermore, the operation pressure for boiling of

water is much less than those for boiling of ethanol and acetone, resulting in much larger bubble size and different boiling regime as shown in Fig. 17. In fact, no intermittent boiling regime exists for boiling of ethanol and acetone. More nucleation sites are activated for acetone and ethanol. As the heat transfer mode for ethanol and acetone is nucleate boiling regime, the heat transfer is steady. Therefore, no instability of boiling heat transfer with ethanol and acetone is observed in the present study.

5. Conclusions

The instabilities of nucleate boiling in a flat evaporator in an evaporator and condenser combined two phase closed system have been investigated thorough careful and systematic experiments and visualisation in the present study. The effects of the heat flux, filling ratio, coolant temperature and working fluid type on the instabilities of nucleate boiling heat transfer and their mechanisms have been explained and analysed according to the experimental data and observations. The following main conclusions have been obtained:

1. In general, the instabilities of nucleate boiling heat transfer are strongly related to the corresponding heat transfer modes at different heat fluxes for boiling of water. Three heat transfer modes: Natural convection, intermittent boiling and fully developed nucleate boiling exist for the test heat flux range in the present study. It has been found that the periodical variation of heat transfer due to the bubble behaviours and physical properties and low operation pressures leads to the instabilities of nucleate boiling heat transfer in the two phase closed system. The maximum intensity of the

fluctuations of evaporator wall temperature and the vapor pressures are 3.1 ^{o}C and 0.8 kPa for distilled water as working fluid at FR=50% and T_{in}=12 ^{o}C.

2. In the flat evaporator and condenser two phase closed system, the condensate droplets may significantly affect the instabilities in the natural convection heat transfer mode due to the inducing of isolated bubble in the liquid at lower heat fluxes but has little effect in intermittent boiling and fully developed nucleate boiling modes at higher heat fluxes.

3. The effects of the filling ratio vary with the heat flux due to the different heat transfer modes. The filling ratio has a significant effect on the instabilities when the heat flux is less than 69.6 W·cm^{-2}, but has little effect when the heat flux is higher than 69.6 W·cm^{-2}. The maximum temperature fluctuation occurs in the intermittent boiling regime.

4. The inlet cooling water temperature has no effect on the temperature fluctuations when the heat flux is less than 23.6 W·cm^{-2}. When the heat flux is higher than 23.6 W·cm^{-2}, the effect of the inlet cooling water temperature becomes obvious. The intensities fluctuations become strong at heat fluxes from 23.6 to 69.6 W·cm^{-2}. At a heat flux higher than 69.6 W·cm^{-2}, the fluctuations become weak as compared to the medium heat fluxes.

5. There is no intermittent boiling regime for boiling of ethanol and acetone in the present study and the fluctuations of evaporator wall temperatures for ethanol and acetone are approximate 0.2 ^{o}C in the present study. The heat transfer mode for

ethanol and acetone is mainly nucleation boiling and fully developed regimes and the heat transfer is steady.

Acknowledgements

This work was supported by the National Natural Science Foundation of China (No. 51576005).

References

[1] A. Faghri, Heat Pipe Science and Technology, Taylor and Francis, Washington D.C., 1995.

[2] A. Niro, G.P. Beretta, Boiling regimes in a closed two-phase thermosyphon, International Journal Heat and Mass Transfer 33 (10) (1990) 2099-2110.

[3] J.F. Liu, J.C.Y. Wang, On the pulse boiling frequency in thermosyphons, Transactions of the ASME 114 (1992) 290-292.

[4] C. Casarosa, E. Latrofa, A. Shelginski, The geyser effect in a two-phase thermosyphon, International Journal Heat and Mass Transfer 26 (6) (1983) 933-941.

[5] P. Griffith, Geysering in liquid-filled lines, ASME Paper 62-HT-39 (1962).

[6] J.A. Boure, A.E. Bergles, L.S. Tong, Review of two-phase flow instability. Nuclear Engineering and Design 25 (2) (1973) 165-192.

[7] K. Negishi, T. Sawada, Heat transfer performance of an inclined two-phase closed thermosyphon, International Journal of Heat and Mass Transfer 26 (8) (1983) 1207-1213.

[8] S.H. Noie, M.R. Sarmastiemami, M. Khoshnoodi, Effect of inclination angle and filling ratio on thermal performance of a two-phase closed thermosyphon under normal operating conditions, Heat Transfer Engineering 28 (4) (2007) 365-371.

[9] T.F. Lin, W.T. Lin, Y.L. Tsay et al., Experimental investigation of geyser boiling in an annular two-phase closed thermosyphon, International Journal of Heat and Mass Transfer 38 (2) (1995) 295-307.

[10] H. Kuncoro, Y.F. Rao, K. Fukuda, An experimental study on the mechanism of geysering in a closed two-phase thermosyphon, International Journal of Multiphase Flow 21 (6) (1995) 1243-1252.

[11] H. Imura, K. Sasaguchi, H. Kozai et al., Critical heat flux in a closed two-phase thermosyphon, International Journal Heat and Mass Transfer 26 (1983) 1181-1188.

[12] M.R. Sarmastiemanmi, S.H. Noie, M.Khoshnoodi, et al., Investigation of geyser boiling phenomenon in a two-phase closed thermosyphon, Heat Transfer Engineering 30 (5) (2009) 408-415.

[13] I. Khazaee, R. Hosseini, S.H. Noie, Experimental investigation of effective parameters and correlation of geyser boiling in a two-phase closed thermosyphon, Applied Thermal Engineering 30 (2010) 406-412.

[14] S.L. Abreu, S. Colle, An experimental study of two-phase closed thermosyphons for compact solar domestic hot-water systems, Solar Energy 76 (1-3) (2004) 141-145.

[15] H. Farsi, J.L. Joly, M. Miscevic, et al., An experimental and theoretical investigation of the transient behavior of a two-phase closed thermosyphon, Applied Thermal Engineering 23 (2003) 1895-1912.

[16] K. Kafeel, A. Turan, Simulation of the response of a thermosyphon under pulsed heat input conditions, International Journal of Thermal Sciences 80 (2014) 33-40.

[17] B. Fadhl, L.C. Wrobel, H. Jouhara, CFD modelling of a two-phase closed thermosyphon charged with R134a and R404a, Applied Thermal Engineering 78 (2015) 482-490.

[18] H. Jouhara, B. Fadhl, L.C. Wrobel, Three-dimensional CFD simulation of geyser boiling in a two-phase closed thermosyphon, International Journal of Hydrogen Energy 41 (2016) 16463-16476.

[19] M. Zhang, Z.L. Liu, G.Y. Ma, et.al., The experimental study on flat heat pipe of magnetic working fluid, Experimental Thermal and Fluid Science 33 (2009) 1100-1105.

[20] H. Hao, J. Li, X. Ling, Study on heat transfer performance of an aluminium flat plate heat pipe with fins in vapor chamber, Energy Conversion and Management 74 (2013) 44-50.

[21] G.M. Zhang, Z.L. Liu, C. Wang, An experimental study of boiling and condensation co-existing phase heat transfer in small confined space, International Journal of Heat and Mass Transfer 64 (2013) 1082-1090.

[22] G.M. Zhang, Z.L. Liu, C. Wang, A visualization study of the influences of liquid levels on boiling and condensation co-existing phase change heat transfer phenomenon in small confined spaces, International Journal of Heat and Mass Transfer 73 (2014) 415-423.

[23] G.M. Zhang, Z.L. Liu, Y.H. Li, et.al., Visualization study of boiling and condensation co-existing phase change heat transfer in a small and closed space with a boiling surface of enhanced structures , International Journal of Heat and Mass Transfer 79 (2014) 916-924.

[24] Y. Tang, J. Zeng, S.W. Zhang, et al., Effect of structural parameters on pool boiling heat transfer for porous interconnected microchannel nets, International Journal of Heat and Mass Transfer 93 (2016) 906-917.

[25] S.W. Zhang, Y. Tang, J. Zeng, et al., Pool boiling heat transfer enhancement by porous interconnected microchannel nets at different liquid subcooling, Applied Thermal Engineering 93 (2016) 1135-1144.

[26] J.R. Taylor, An Introduction to Error Analysis, second ed., University Science Books, 1997.

[27] M.G. Cooper, Saturation nucleate pool boiling-a simple correlation, Institution of Chemical Engineers Symposium Series 86 (2) (1984) 785-793.

List of Table Captions

List of Figure Captions

Fig. 11. Variations of the several temperatures and pressure of the two phase closed test section for water boiling at q = 80.2 W·cm^{-2}.

Fig. 12. Variations of HTC and ΔT at q = 80.2 W·cm^{-2}.

a: HTC versus time.

b: T_w versus time.

Fig. 13. Images of fully developed boiling at q = 80.2 W·cm^{-2}.

Fig. 14. *SD* of T_w versus heat flux for water at different filling ratios.

Fig. 15. *SD* of T_w versus heat flux at three inlet cooling water temperatures for water at *FR* = 50%.

Fig. 16. Effects of the working fluid types on the nucleate boiling heat transfer

a: *SD* of T_w versus heat flux for three different working fluids.

b: Boiling curves for three different working fluids.

c: Experiment data compared with the Cooper correlation.

Fig. 17. Comparison of the bubbles size and nucleation site density with three working fluids at different heat fluxes.

a: Typical images for bubbles behavior at q = 38.7 W·cm^{-2} during a growth period.

b: Typical images for bubbles behavior at q = 80.2 W·cm^{-2}.

Table 1. Thermal properties of three working fluids at sub-atmospheric pressure.

Fluids	T_{sat} (^{o}C)	P_{sat} (kPa)	ρ_l (kg·m^{-3})	ρ_v (kg·m^{-3})	h_{fg} (kJ·kg^{-1})	C_p (kJ·kg^{-1}·K^{-1})	k_l (W·mK^{-1})	σ (mN·m^{-1})
Water	20	2.3393	998.16	0.01731	2453.49	4.1844	0.5984	72.736
Ethanol	20	5.9245	789.59	0.11241	926.61	2.5121	0.1663	22.414
Acetone	20	24.662	790.19	0.60104	539.22	2.1311	0.1572	23.678

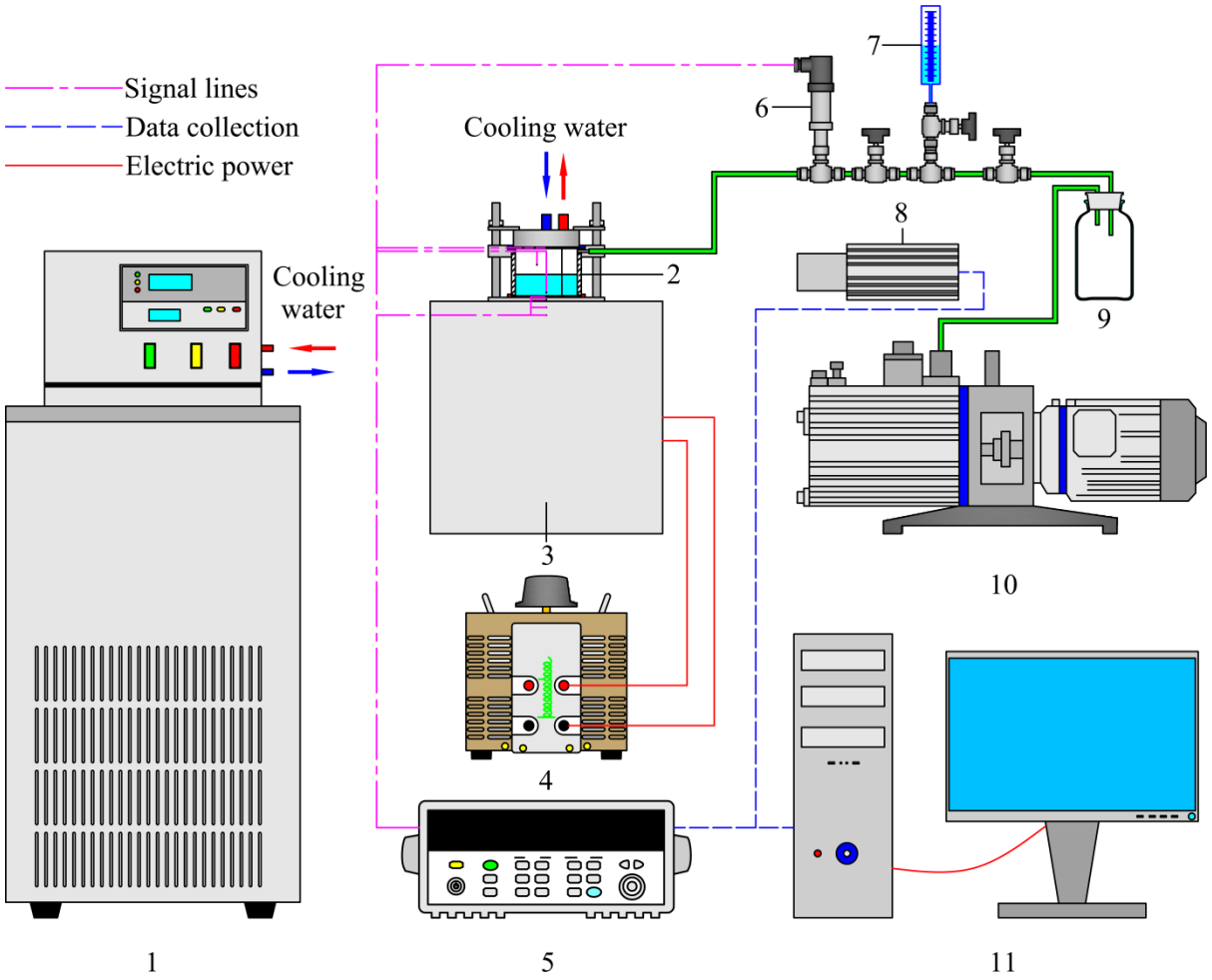

1: chiller; 2: test section; 3 heating unit; 4: voltage regulator; 5: data acquisition/switch unit; 6: pressure sensor; 7: reservoir; 8: high speed camera; 9: drainage bottle; 10: vacuum pump; 11: PC.

Fig. 1. Schematic diagram of the experimental system.

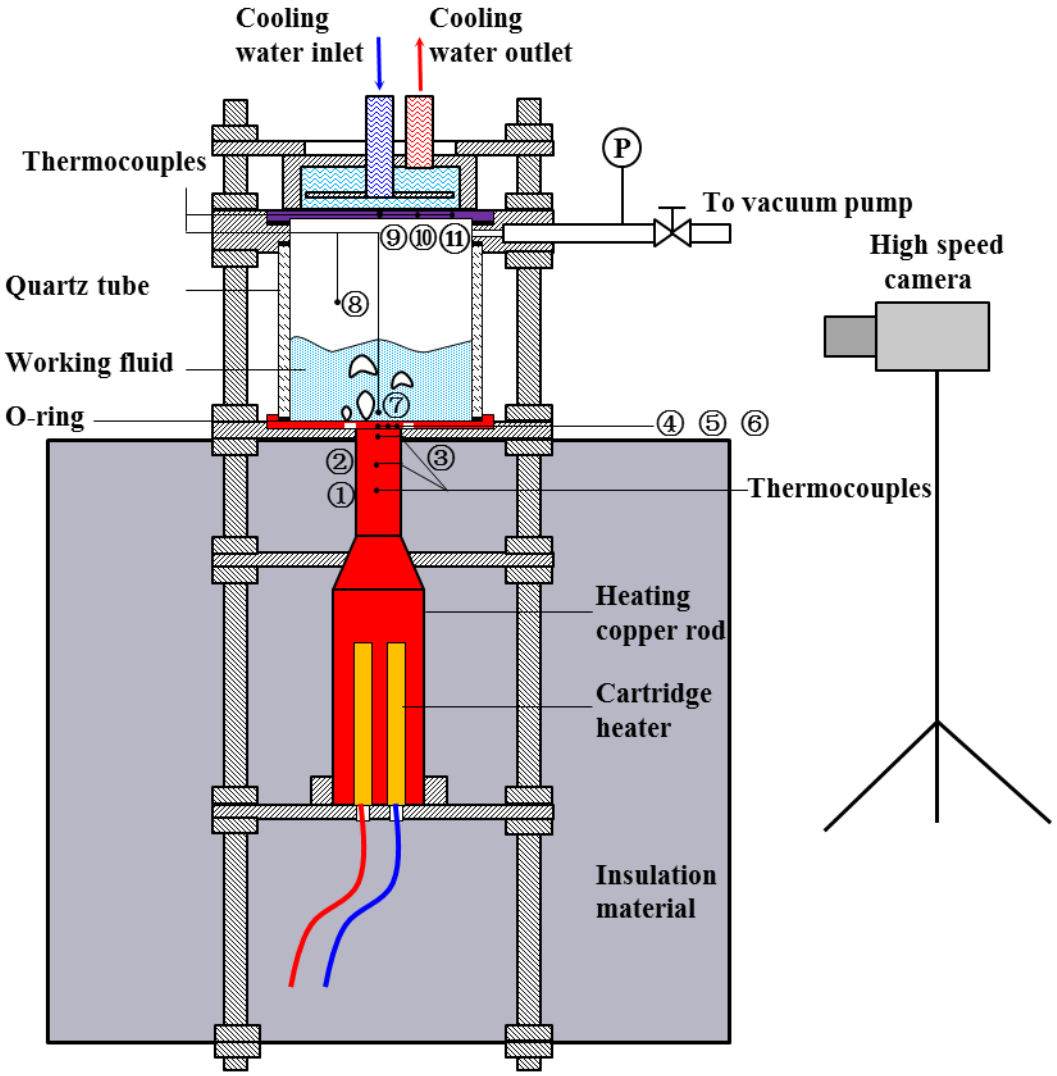

Fig. 2. Schematic diagram of heating unit and the test section.

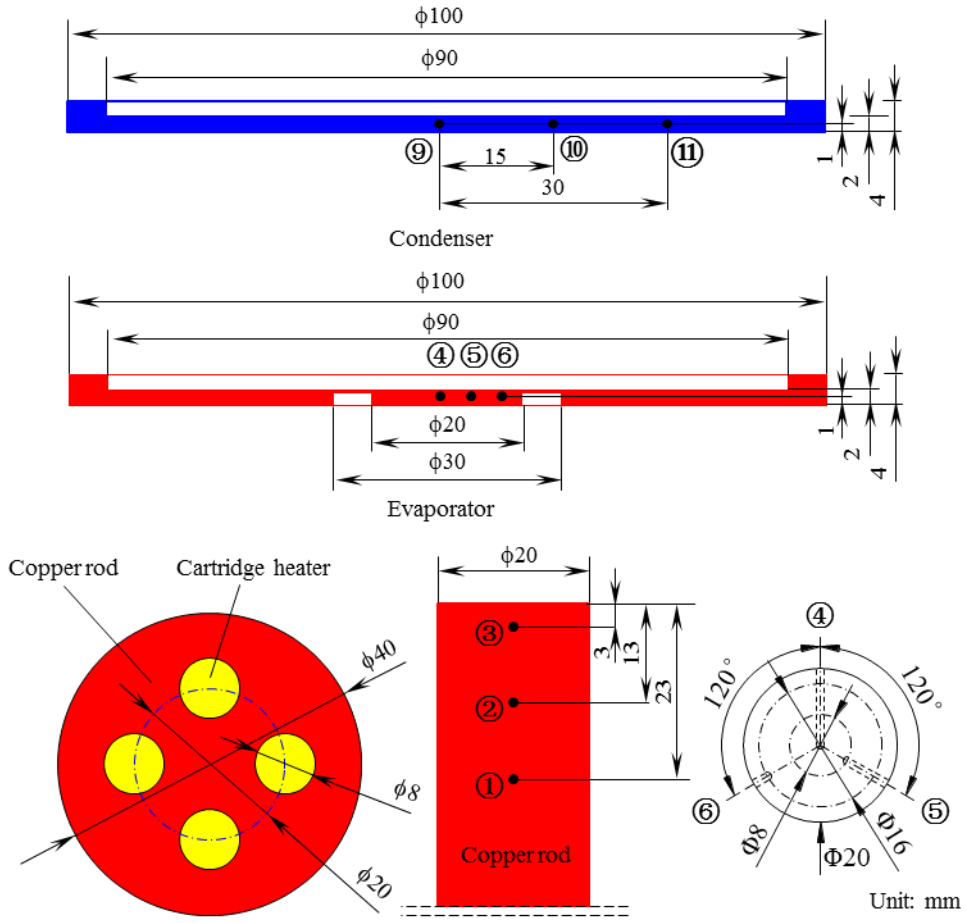

Fig. 3. Details of the copper block, evaporator and condenser.

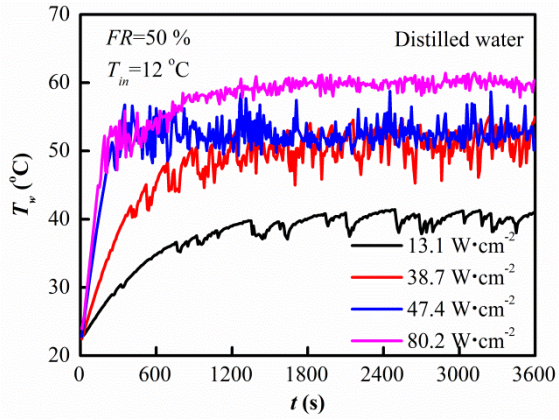

Fig. 4. T_w response for different heat fluxes.

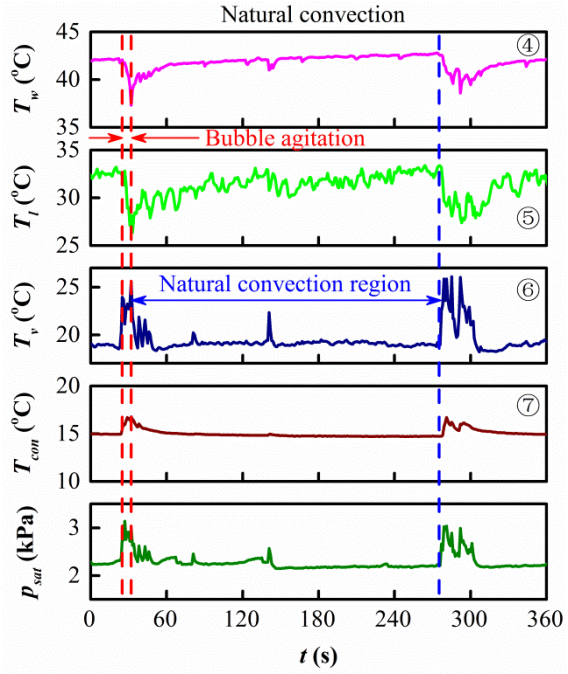

Fig. 5. Variations of the several temperatures and pressure of the two phase closed test section for water at q = 13.1 W·cm^{-2}.

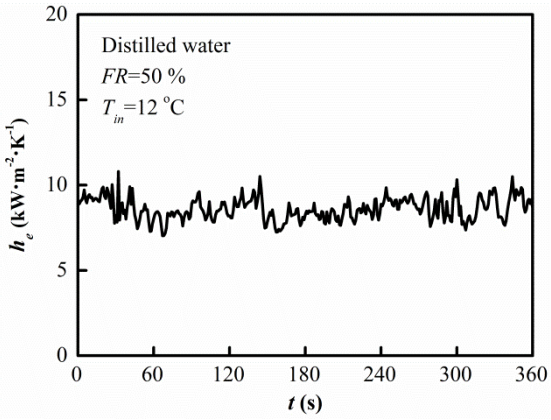

a: HTC versus time.

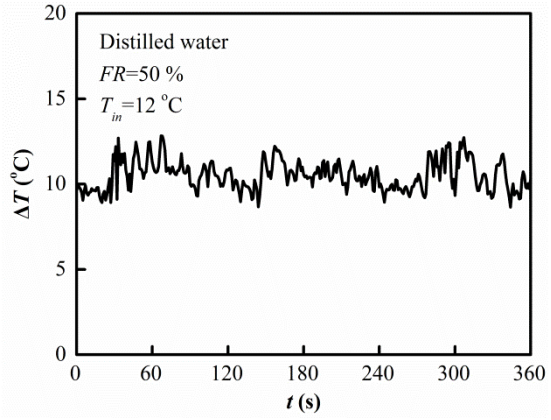

b: ΔT versus time.

Fig. 6. Variations of HTC and ΔT at q = 13.1 W·cm^{-2}.

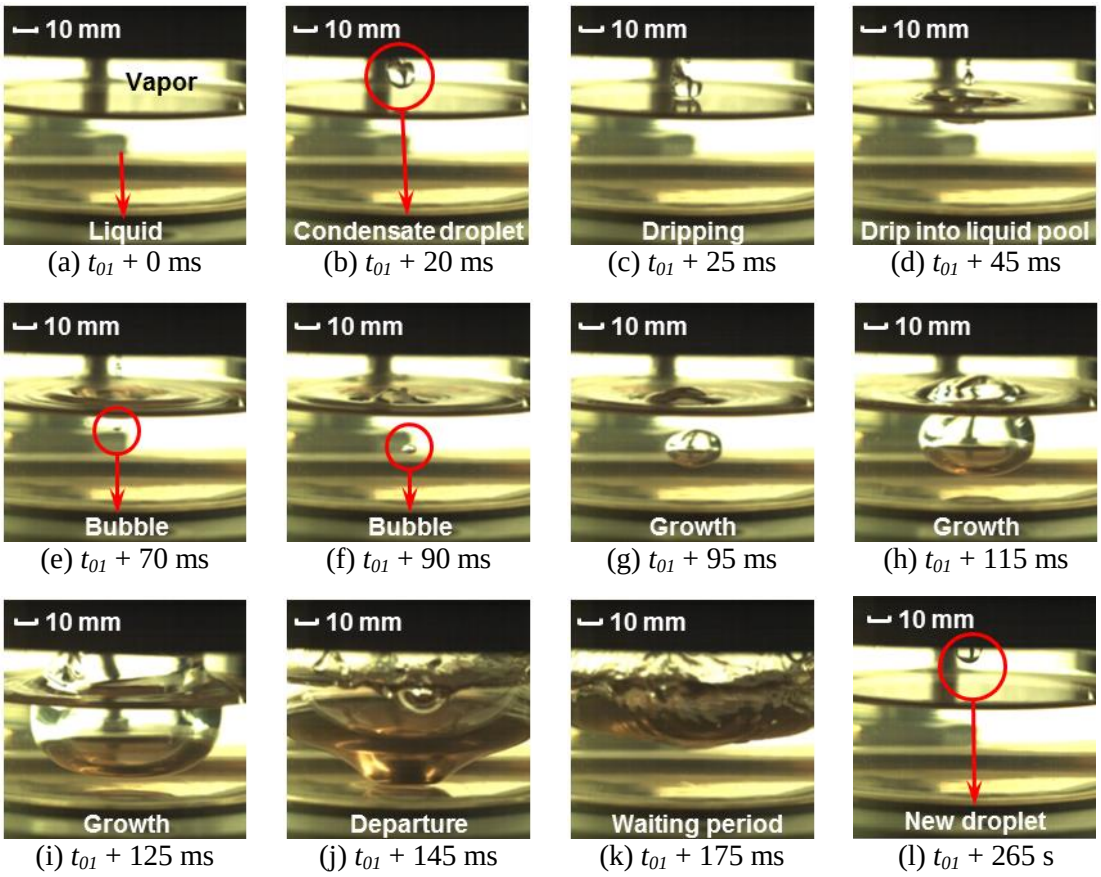

(a) t_{01} + 0 ms (b) t_{01} + 20 ms (c) t_{01} + 25 ms (d) t_{01} + 45 ms

(e) t_{01} + 70 ms (f) t_{01} + 90 ms (g) t_{01} + 95 ms (h) t_{01} + 115 ms

(i) t_{01} + 125 ms (j) t_{01} + 145 ms (k) t_{01} + 175 ms (l) t_{01} + 265 s

Fig. 7. Images of boiling incipience caused by the drippings of condensate at q = 13.1 W·cm^{-2}.

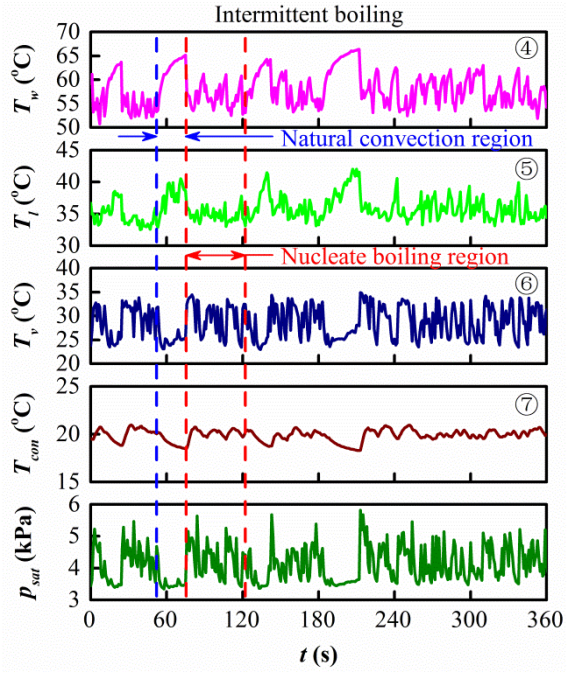

Fig. 8. Variations of the several temperatures and saturated pressure of the two phase closed test section for water at q = 38.7 W·cm^{-2}.

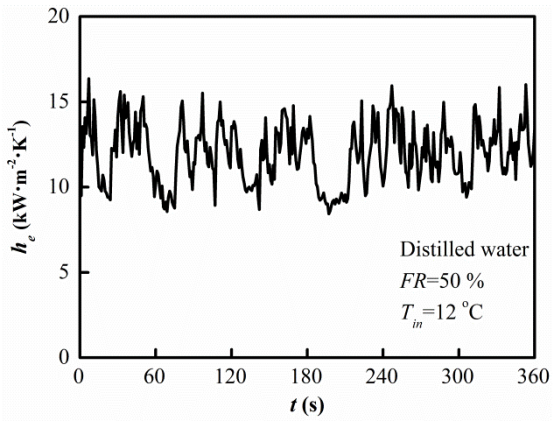

a: HTC versus time.

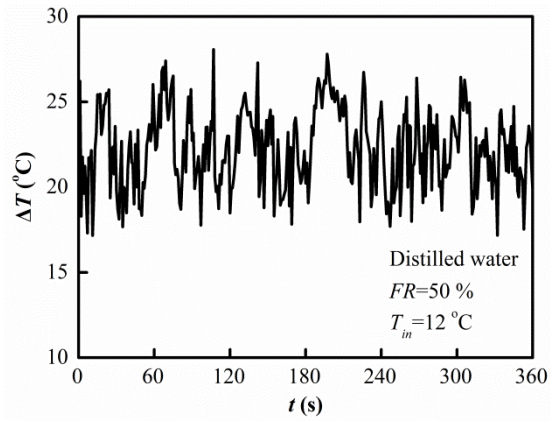

b: ΔT versus time.

Fig. 9. Variations of HTC and ΔT at q = 38.7 W·cm^{-2}.

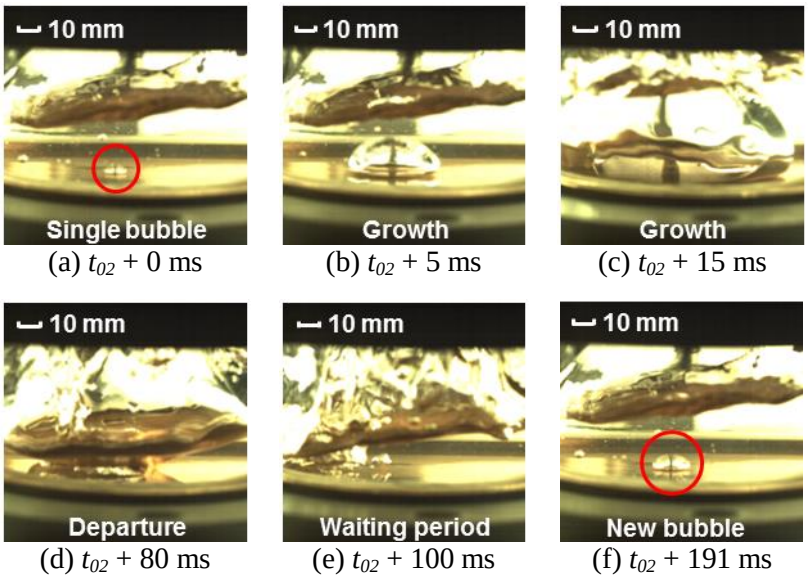

(a) t_{02} + 0 ms (b) t_{02} + 5 ms (c) t_{02} + 15 ms

(d) t_{02} + 80 ms (e) t_{02} + 100 ms (f) t_{02} + 191 ms

Fig. 10. Visualization of intermittent boiling at q = 38.7 W·cm^{-2}.

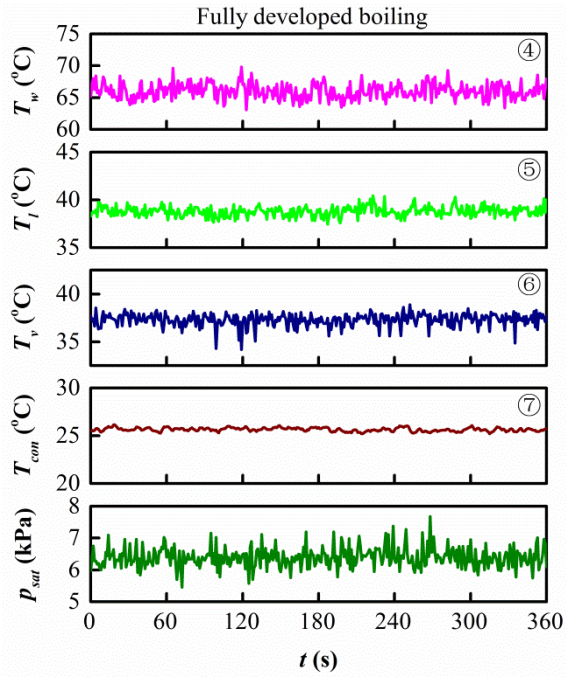

Fig. 11. Variations of the several temperatures and saturated pressure of the two phase closed test section with time for water at q = 80.2 W·cm^{-2}.

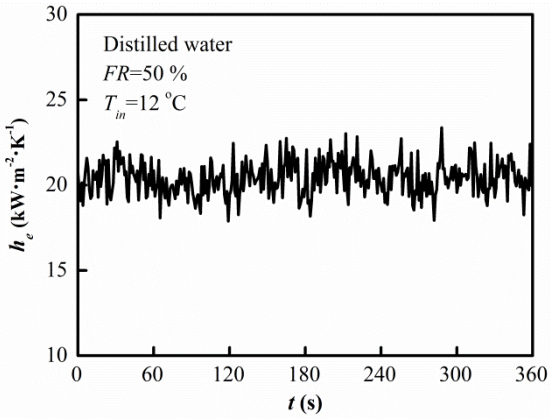

a: HTC versus time.

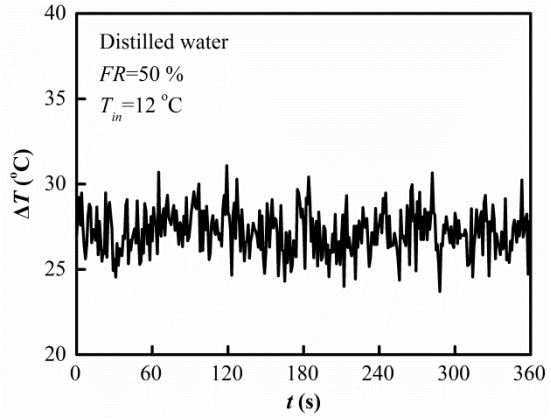

b: ΔT versus time.

Fig. 12. Variations of HTC and ΔT at q = 80.2 W·cm^{-2}.

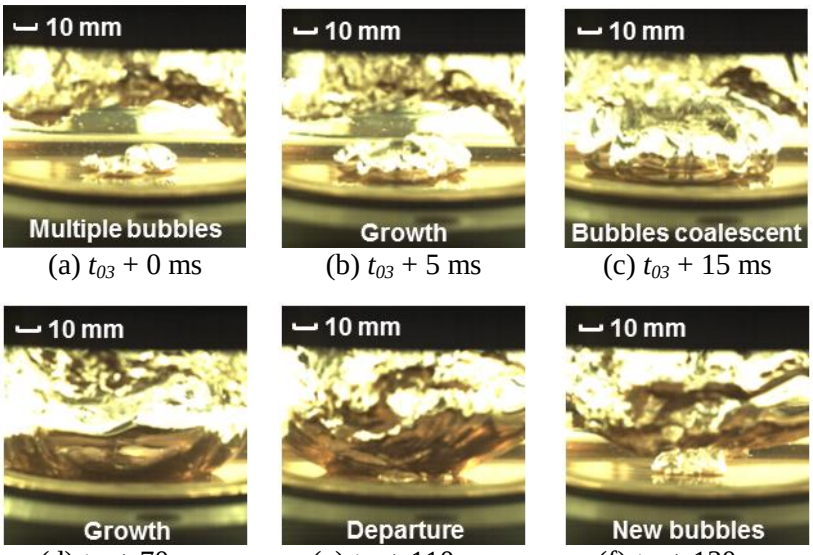

(a) t_{03} + 0 ms (b) t_{03} + 5 ms (c) t_{03} + 15 ms

(d) t_{03} + 70 ms (e) t_{03} + 110 ms (f) t_{03} + 130 ms

Fig. 13. Images of fully developed boiling at q = 80.2 W·cm^{-2}.

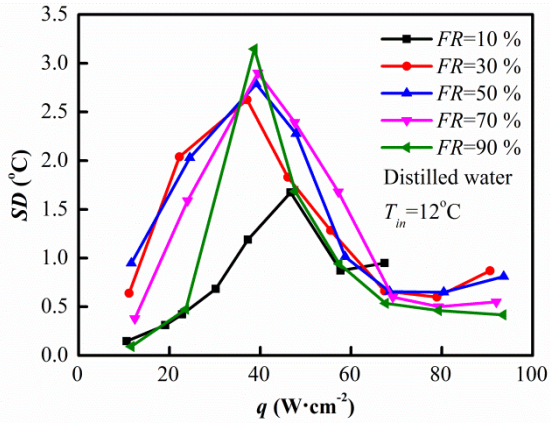

Fig. 14. *SD* of T_w versus heat flux for water at different filling ratios.

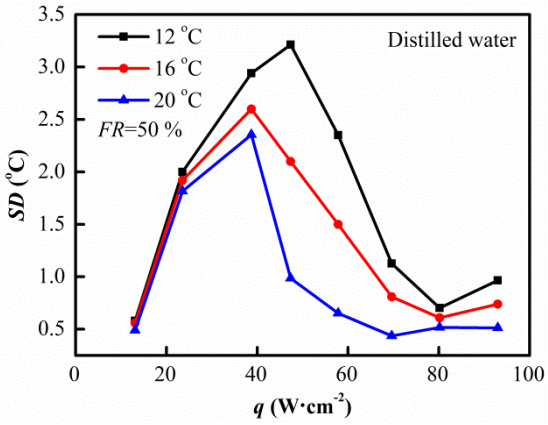

Fig. 15. *SD* of T_w versus heat flux at three inlet cooling water temperatures for nucleate boiling of water at *FR* = 50%.

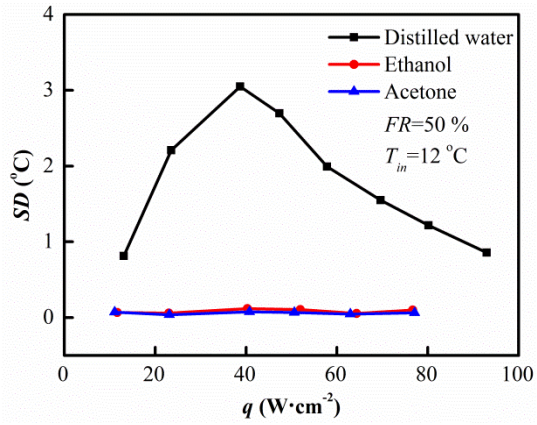

a: *SD* of T_w versus heat flux for three different working fluids.

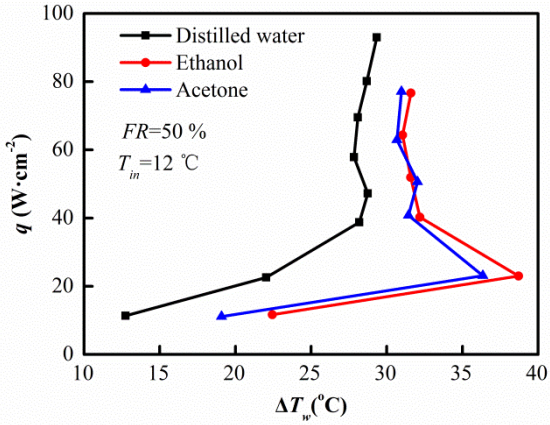

b: Boiling curves for three different working fluids.

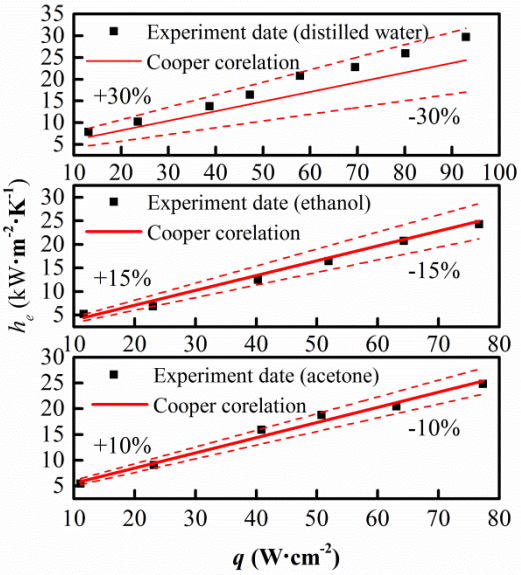

c: Experiment data compared with the Cooper correlation.

Fig. 16. Effects of the working fluid types on the nucleate boiling heat transfer

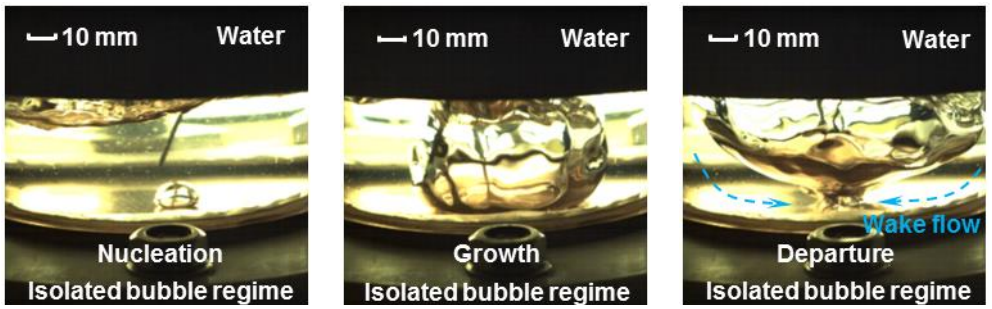

(a) t_{04} + 0 ms (b) t_{04} + 25 ms (c) t_{04} + 75 ms

A life time of isolated bubble from nucleation to departure

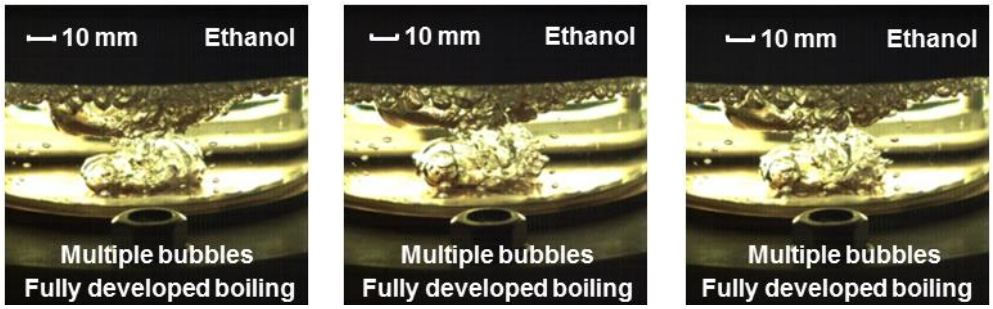

(a) t_{05} + 0 ms (b) t_{05} + 10 ms (c) t_{05} + 15 ms

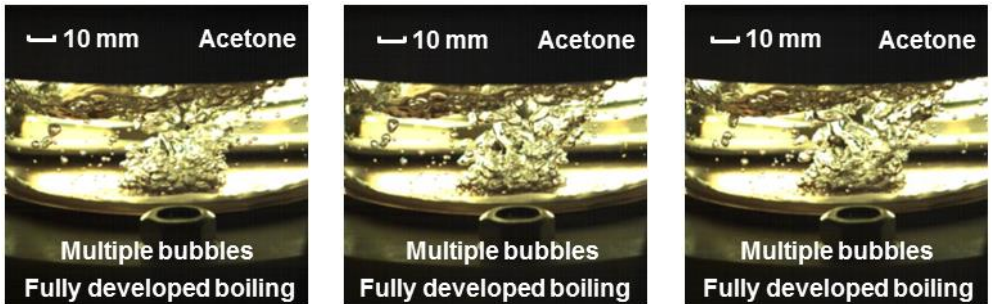

(a) t_{06} + 0 ms (b) t_{06} + 5 ms (c) t_{06} + 10 ms

a: Typical images for bubbles behavior at q = 38.7 W·cm^{-2} during a growth period.

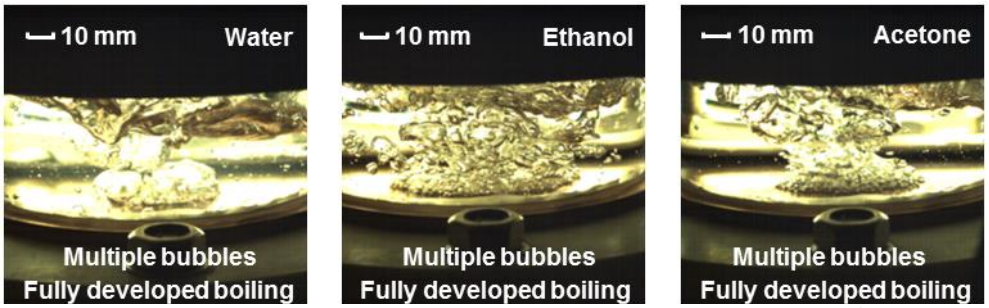

b: Typical images for bubbles behavior at q = 80.2 W·cm^{-2}.

Fig. 17. Comparison of the bubbles size and nucleation site density with three working fluids at different heat fluxes.